CHARACTERIZATION OF O_2 CONTENT IN 3D ORGANOID CULTURE MODELS

by

Shyanne Grace Salen

A thesis submitted to Johns Hopkins University in conformity with the requirements for the degree of Master of Science in Engineering

Baltimore, Maryland

June 2020

Abstract

Breast cancer is the most common cancer in women and the second leading cause of female cancer-related deaths. Low oxygen tension (hypoxia) arises in most solid tumors due to the imbalance of oxygen supply and consumption. Hypoxia is an adverse prognostic marker in various cancer types. Recently, the Gilkes lab developed a hypoxia fate-mapping system, which permanently marks hypoxic cells to enable the mapping of their fate during tumorigenesis. This dual lentiviral vector system was transduced into MDA-MB-231 cells, which permanently switch from DsRed to GFP when exposed to hypoxia. In a parallel study, a hypoxia fate-mapping transgenic mouse model forms spontaneous breast tumors, whose cells permanently switch from TdTomato to GFP expression under hypoxia. We utilized this model to produce a three-dimensional cell culture that allows for better recapitulation of the tumor microenvironment, but the extent of oxygen diffusion through the 3D matrices is poorly understood.

We investigated the O_2 content in 3D matrices using organoids generated from the breast tumors of the triple transgenic mouse model. First, these organoids were exposed to normoxia and hypoxia to determine the most sensitive mouse model: EF1-CREODD(+/-)TdTm(+/+). Next, to characterize our model, organoids, embedded in Matrigel, demonstrated an inverse correlation between exposed O_2 conditions and GFP expression. At 20% O_2, organoids embedded in Matrigel formed GFP+ hypoxic cores; however, organoids cultured in collagen presented a more invasive phenotype where hypoxic cores did not develop. Then, the O_2 depletion of organoids with varied cell density, scaffold material, and cell activity was measured using OXNANO nanoprobes. For organoids cultured in Matrigel, the O_2 levels decreased with increasing seeding density, while the collagen embedded organoids remained constant over the 10-day time-course.

Finally, O_2 depletion was measured in hypoxia fate-mapping MDA-MB-231 derived spheroids embedded in Matrigel, where the O_2 level decreased with increasing initial cell density. Our work suggests that Matrigel is a better platform to study growth and spontaneous hypoxia, whereas collagen is better for invasion studies. Nevertheless, more work is warranted into the hypoxic core formation to develop a reproducible 3D tumor model that recapitulates the tumor microenvironment to better understand hypoxia in cancer.

Primary Reader and Advisor: Dr. Daniele Gilkes

Secondary Reader: Dr. Stavroula Sofou

Acknowledgments

First, I would like to thank my advisor, Dr. Daniele Gilkes, for giving me the opportunity to work in her lab and for her insight and guidance throughout my pursuit of the Masters of Science in Chemical and Biomolecular Engineering degree. Additionally, I would like to thank Dr. Stavroula Sofou for agreeing to be my second reader for this thesis.

In addition, I owe my gratitude to everyone in the Gilkes lab for all the encouragement and fun times throughout the past two years. I truly could not have asked for a better group of people to work in the lab with every day. I would especially like to acknowledge Inês Godet for all her advice, help, and guidance throughout this whole process. Additionally, I would like to thank Josh DiGiacomo and Mahelet Mamo for always being there for support and a laugh during challenging times. I really appreciate the experience of being able to work alongside these intelligent and passionate scientists.

Table of Contents

List of Tables

List of Figures

Chapter 1

Introduction

1.1 Breast Cancer

Breast cancer is the most prevalent cancer in women. The American Cancer Society estimates there will be 276,000 new cases of breast cancer for females in the United States in 2020, equating to approximately 30% of all cancer incidences[1]. Likewise, 12.8% or 1 in 8 women will develop breast cancer in her lifetime[1]. Furthermore, breast cancer is the second leading cause of cancer-related deaths with more than 42,000 deaths estimated for 2020, representing 15% of cancer deaths in women[1]. Although the number of breast cancer deaths declined by 40% from 1989 to 2017, the death rate stabilized in recent years after more than two decades of decline[2]. Breast cancer mortality is mostly caused by metastasis, equating to 90% of all cancer attributed deaths[2]. Consequently, the five-year survival rate is 90% for all breast cancer, but drops to 27% for metastatic breast cancer[1]. Primary tumors can be successfully removed via surgery or treated with radiation, but after the cells disseminate to distant organs in the body, these metastases are very difficult to treat. Despite the advancements in cancer diagnosis and treatment, there is still no techniques for definitively identifying patients who will metastasize or relapse[2].

Metastasis is the least understood process of tumorigenesis. Tumor cells must acquire a motile phenotype for the initiation process to begin, which is mediated by a process called the epithelial mesenchymal transition (EMT). Formation of new blood vessels is essential for further growth and allows tumor cell dissemination at distance sites[3]. Then, the cell can detach from the primary vascularized tumor, invade the surrounding tissue, intravasate into nearby blood vessels,

and circulate in the vascular system[4]. Some of the circulating tumor cells (CTCs) in the vascular system adhere to blood vessel walls. These cells are able to extravasate and migrate into the local tissue, where they can colonize in sites such as the brain, bone, lung, and liver in the case of breast cancer. There has been an increasing amount of evidence revealing oxygen (O_2) content of tumor tissue as an important determinant of metastasis.

1.2 Hypoxia

Most solid tumors, larger than 1 mm^3, contain hypoxic regions because of the inability to provide the growing tumor mass with adequate amounts of O_2[3]. These regions develop in 90% of solid cancers[5]. Hypoxia (low oxygen tension) and anoxia (no measurable oxygen) arise due to an imbalance between oxygen supply and consumption[6]. In normal tissues, the O_2 supply matches the metabolic requirements; however, in solid tumors, the elevated proliferation causes an increased consumption rate that may outweigh the insufficient oxygen supply, resulting in regions of hypoxia[7]. There are two types of hypoxia: acute and chronic[8]. Acute, or ischemic hypoxia, is perfusion-limited oxygen delivery due to abnormal vasculature network and high interstitial pressure, resulting in abnormal blood flow, which is often transient[9]**.** Chronic hypoxia is diffusion-limited hypoxia, which is caused by large diffusion gradients created by the high proliferation rate of cancer cells, inadequate blood vessel formation, and adverse diffusion geometry[5,7]. Solid tumors arise without existing vasculature and the new inadequate blood vessels that form are leaky and have chaotic architecture and non-laminar blood flow[10]. The oxygen diffuses 100-200 μm away from the nutritive blood vessels, depending on the local oxygen concentration in the blood and the rates of oxygen consumption of the surrounding cells[1,6]. Hypoxic regions occur approximately 200 μm away from blood vessels[10]. The degree of

hypoxia experienced by a cell is determined by its proximity to the arterial blood supply and rates of O_2 consumption by the neighboring cells[11]. Farther from the blood vessels, necrosis develops as a direct result of limited oxygen and nutrients, suggesting that given sufficient time hypoxic cells will become necrotic[12].

The hypoxic environment in tumors selects for cells that respond and adapt to oxygen deficiency[10]. Cells require an adequate and continuous supply of oxygen to use as the terminal electron acceptor for the process of mitochondrial respiration, which generates ATP[13]. Hypoxia leads to insufficient oxygen for efficient ATP production so the hypoxic tumor cells turn to anaerobic glycolysis to meet their energetic demand[9,10,14]. Similarly, tumor cells respond to low levels of oxygen with distinct changes in gene expression that promote cell survival and tumor progression. These pathways are involved in cell proliferation, angiogenesis, apoptosis, metabolism, and inflammation[9,15].

1.2.1 Hypoxia and Breast Cancer

Several studies indicate low oxygen tension in tumors is an adverse prognostic marker in various cancer types[3,9,16]. Notably, 25-40% of invasive breast cancer exhibits hypoxic regions[17]. On average, the partial pressure of oxygen (pO_2) in normal human breast tissue is 65 mmHg (~8.5% O_2), while breast tumors have a range of 2.5 to 28 mmHg (0.3-3.6% O_2)[18]. Patients with a pO_2 of less than 10 mmHg are at an increased risk of metastasis and mortality[19]. Hypoxic tumors are found to correlate with metastatic occurrences and a number of studies demonstrate an inverse correlation between tumor oxygenation and clinical outcome[8–10,16]. Hypoxic cells have reduced drug delivery for chemotherapy, intrinsic radioresistance, apoptosis resistance, a pro-

angiogenic phenotype, and enhanced metastatic capacity, which contribute to the observed poor outcome[3].

1.2.2 Hypoxia-inducible-factor

The most well-characterized hypoxia response pathway is mediated by the hypoxia-inducible factors (HIFs). HIFs (HIF-1 and HIF-2) permit tumor cells to adapt by facilitating oxygen delivery and adaptation to oxygen deprivation by inducing hypoxia responsive genes[20,21]. HIF-1 is a heterodimeric transcription factor consisting of an oxygen regulated, HIF-1α, and, a constitutively expressed, HIF-1β/ARNT (aryl hydrocarbon receptor nuclear translocator)[18,22]. HIF-1α expression is precisely regulated by cellular O_2 concentration. In normoxia, HIF-1α is polyubiquitinylated and targeted for proteasomal degradation[22]. HIF-1α contains an oxygen-dependent degradation domain within which there is a binding domain for the tumor suppressor von Hippel-Lindau protein (pVHL)[3]. Under normal oxygen conditions, prolyl hydroxylase domain (PHD) proteins hydroxylate HIF-1α[23]. After hydroxylation, pVHL organizes the assembly of a complex that activates the E3 ubiquitin ligase which then ubiquitinylates HIF-1α, targeting for proteasomal destruction[3]. Conversely, during hypoxia, the unmodified HIF-1α no longer interacts with pVHL, PHD enzymes lose their activity, and the active form of HIF-1 accumulates[15].

Hypoxia results in the rapid accumulation of HIF-1α to the nucleus where it dimerizes with HIF-1β and leads to the transcriptional activation of hundreds of target genes by binding to a DNA sequence termed the hypoxia -responsive element (HRE)[22,23]. Three hours of hypoxia *in vitro* is sufficient time to observe HIF-1α stabilization in cancer cells[23]. However, after a few days, there is a decrease in HIF-1α to lower expression levels. Similar to HIF-1α, HIF-2α is also

regulated by oxygen-dependent hydroxylation. HIF-1α and HIF-2α are structurally similar in DNA binding and dimerization domains, but differ in their transactivation domains[24]. Under hypoxia, HIF-2α also dimerizes with HIF-1β and in general, regulates similar genes to HIF-1α[20].

Stabilization of HIFs are correlated with poor clinical outcomes, high mortality rates, chemoresistance, and metastasis in several types of cancer[10,23]. These transcription factors induce the expression of genes that contribute to metabolic reprogramming, angiogenesis, and changes in apoptosis[5,25]. HIFs also contribute to metastasis through the downregulation of adhesion molecules and the increase in motility by regulating EMT as well as inducing cell migration and invasion through matrix degrading enzymes[15]. HIF-1α over expression in tumor biopsies is correlated with increased patient mortality in breast cancer[23]. Similarly, HIF-2α is associated with distant recurrence and poor outcome[6]**.** Although studies indicate that intratumoral hypoxia and increased HIF-1α expression are associated with aggressive cancers, the ability to identify patients at risk is still limited[21].

1.3 Oxygen Characterization

The detection of the extent of tumor hypoxia could potentially enable appropriate patient classification and allow clinicians to make informed decisions regarding the therapy management for the patient[26]. Current methods for gauging tumor hypoxia are to directly measure O_2, assess physiologic processes involving oxygen molecules, and evaluate the expression of endogenous markers[26]. The direct measurement of O_2 in human tumor tissue has been performed using polarographic needle electrodes or fiber-optic probes, but with these methods, the individual cells cannot be visualized or separated[9,27]. Indirect O_2 measurements have been performed using immune labeling of endogenous markers, such as transcriptional

targets of HIFs, and by using chemical hypoxia probes such as pimonidazole[9,27]. Furthermore, clinical methods include magnetic resonance spectroscopy, X-ray imaging, optical imaging, and positron emission tomography[9,27,28].

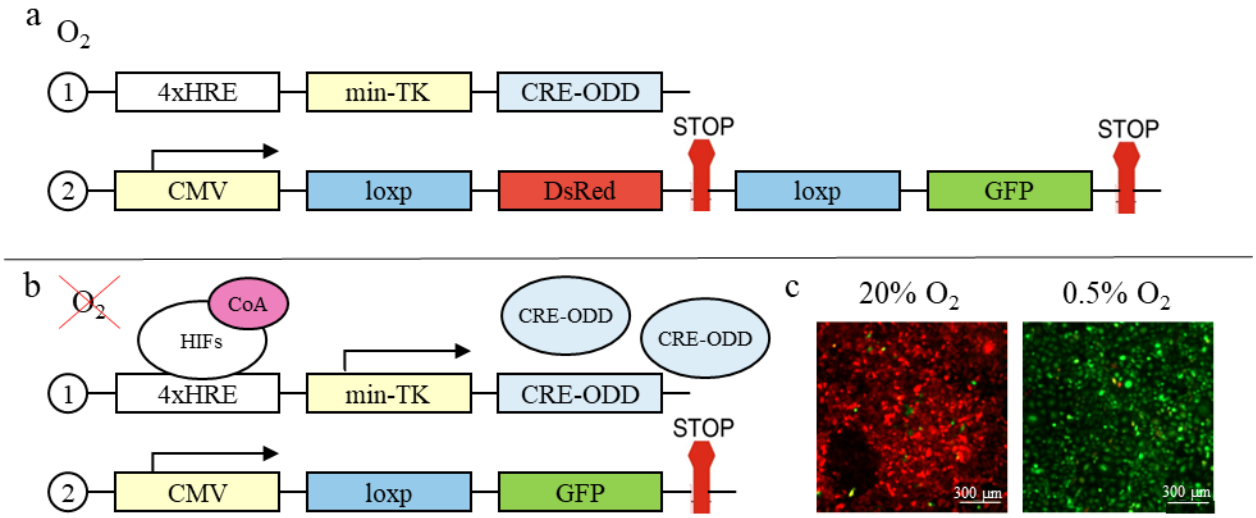

Figure 1: Hypoxia fate-mapping MDA-MB-231 cell line a. The Gilkes lab developed two lentiviral vectors that were used to generate a hypoxia fate-mapping MDA-MB-231 cell line. Under normoxic conditions, DsRed is constitutively expressed. b. Under hypoxic conditions, the expression of the Cre enzyme results in the cleavage of DsRed from vector 2 causing the expression of GFP. c. Fluorescent images of MDA-MB-231 hypoxia fate-mapping cells after exposure to 20% and 0.5% O_2 conditions for 11 days.

1.4 Hypoxia Fate-Mapping System

Recently, the Gilkes lab developed a hypoxia fate-mapping system, which permanently marks hypoxic cells and enables the mapping of their fate during tumorigenesis[29]. This dual-vector system can be used to track hypoxic cells that undergo reoxygenation during metastasis. The first vector contains 4 HIF-DNA binding sequences (HRE), which transcriptionally controls a Cre gene modified with an oxygen-dependent degradation domain (ODD) (Fig. 1). The second vector has a constitutively active promoter (CMV) followed by a red fluorescent reporter protein (DsRed) with a stop codon flanked by tandem loxP sites followed by eGFP, a green fluorescent protein (Fig. 1). Under normal oxygen conditions, the cells express DsRed (Fig. 1a). However, under hypoxia, HIF stabilization causes binding to the repetitive HRE sequences, which ensure

an irreversible DsRed to GFP reporter switch, and the transcription of CRE-ODD, leading to the cleavage of DsRed and permanent GFP expression (Fig. 1b). Our system is tightly controlled to low O_2 levels (<0.5%) and does not change under physiological conditions that mimic normal breast tissue (8% O_2) (Fig. 1c).

1.5 Two- versus Three-dimensional Cell Culture

Cell culture is essential for modern biomedical research to improve our understanding of tissue morphology, cell biology, and mechanisms of disease[29–31]. In cancer research, cell culture and mouse models are the primary tools used to understand tumor biology and optimize treatments. Two-dimensional (2D) cell cultures are the most utilized and consist of primary cell cultures and established cell lines deposited in cell banks. Primary cell cultures have difficulties with isolation and short life span, while established cell lines do not capture the true variety between cancer types[30]. The advantages of working with cell lines is that they are homogenous, simple to grow and propagate, and allow for high-throughput screenings[32]. The major challenges with 2D cultures are potential changes of cell morphology, method of division, and a loss of phenotype[30,33]. Cell cultures in 2D grow on a monolayer attached to glass or plastic dishes, where they are exposed to an unlimited and uniform source of oxygen and nutrients[30]. Additionally, 2D cell cultures lack variability of nutrients, genetic heterogeneity, and the interaction with matrix protein and other cell types[34]. Conversely, mouse models capture heterogeneity, but do not allow for high throughput screening.

Three-dimensional models could be the intermediate between 2D and animal studies. Using 3D cultures may allow for better recapitulation of tumor environments, leading to a better understanding of cancer biology and treatment options. Cells can be cultured in 3D by

suspension in concentrated medium or gel-like substances, or on a scaffold[30]. Moreover, studies have shown that there are great similarities between the morphology and behavior of cells in a tumor mass and those in 3D culture conditions[30]. Markedly, cells cultured on ECM restore some mammary specific gene expression[35]. The main challenges with 3D cultures are that they are less efficient, have a shorter life-span, and have more difficult repeatability when compared to 2D cultures[36]. Additionally, 3D cultures increase complexity for imaging, analysis, and quantification[37]. These models are generated using cellular spheroids, organoids, multilayered cultures of cancer cells, or tumor slices embedded in various matrices[33].

1.5.1 Matrices used in 3D Culture

Natural materials, such as collagen, hyaluronic acid, and chitosan, and synthetic materials, such as, polyethylene glycol, poly(lactic-co-glycolic) acid, and polycaprolactone have been used in 3D cell cultures. Natural materials are more variable and expensive to manufacture than engineered synthetic materials. These materials are used to construct scaffolds to physically support cell adhesion and growth as well as promote self-assembly of cells into 3D clusters[33]. For instance, two major matrices used in 3D cultures are collagen type I and Matrigel. Fibrillar collagen I, a main structural protein in mammary glands, plays an important role in the development of breast cancer[38]and is commonly used to study 3D migration of many cell types[38].

Matrigel is a basement-membrane-like matrix, which is a complex mixture of over 1000 proteins, rich in collagen type IV, laminin, and nidogen[33,35]. The advantages of Matrigel are its ease of handling, fast gelling kinetics, and readily available production with high quality control[33]. However, Matrigel has some limitations, such as lack of control of formulation and

gelation kinetics[33]. Additionally, Matrigel could have issues with reproducibility due to inconsistent composition and batch-to-batch variability.

1.5.2 Spheroid Model

Spheroids are the simplest *in vitro* model of solid tumors and are generated using cancer cell lines. Epithelial cancer cells form intercellular adhesions and self-assemble into compact clusters on nonadherent surfaces or within a 3D matrix. The 3D morphology of spheroids establishes close cell-cell and cell-matrix adhesions[33]. Moreover, the spheroids experience nonuniform concentrations of oxygen and nutrients, which can lead to oxygen gradients, causing hypoxic cores in the center of the spheroid[31,33]. Spheroids can be cultured in suspension or in collagen, Matrigel, and synthetic scaffolds, which allow the study of migration and invasion. Spheroids have the advantages of well-defined geometry, cell-cell and cell-ECM interactions, and reproducibility[37]. The simplicity and increased tumor mimicry of spheroids promotes the ability to conduct high throughput drug screening, basic tumor growth studies, and analysis of cellular responses to chemical compounds[33]. However, spheroids are formed from established cancer cell lines, which neglect to capture the complexity and heterogeneity of tumors. To overcome this limitation, organoid models may provide more heterogeneity and better recreation of the tumor microenvironment.

1.5.3 Organoid Model

Organoids, created from both normal and tumor tissue, can recapitulate the epithelial architecture and physiology of tissues[36]. When formed from the tumor mass, organoids closely model the *in vivo* tumor characteristics and genetic heterogeneity, which are preserved in culture over

time[34,39]. Organoid cultures provide an attractive platform to test new drug treatments. Additionally, multiple organoids can be generated from a single biopsy, facilitating high-throughput tests of multiple and a combination of drugs using a small amount of tissue[40]. However, organoid models do not entirely recreate a tumor in a 3D environment because they still lack stroma, blood vessels, and immune cells[34]. Unlike spheroid cultures, organoids are mainly encapsulated in natural biomaterials, such as Matrigel and collagen. Matrigel embedment is the most commonly used structure for organoid cultures[33]. Breast cancer organoids in Matrigel form important features of epithelial development of the ductal microenvironment[38]. Consequently, cancer organoids could fill the gap between cancer cell lines and mouse models because of their physiological relevance and ability for creating high-throughput screens[32].

1.5.4 Oxygen and 3D Cultures

The conditions in which cells are cultured can greatly affect the observed biology and reproducibility. Oxygen, which is often ignored, could develop gradients, especially in 3D cultures. Oxygen diffusion through 3D cultures is limited because it must diffuse from the gas and liquid phases through the solid phase of cell clusters, extracellular matrix, and hydrogels[41]. Due to convenience, tumors cells are typically cultured at hyperoxic conditions well above the pO_2 of human tissues. The air in a cell culture incubator contains 140 mmHg O_2 (18.5%)[31]. In particular, 3D cell cultures experience concentration gradients as a result of the competition between diffusion and consumption[35]. Notably, considering its relatively low solubility in culture medium, oxygen is usually the most easily depleted[35].

1.6 Motivation

Hypoxia has been shown to be a negative prognostic factor for solid tumors. Chemoresistance is a major factor in the poor clinical outcome of hypoxic tumors. Notably, up to 95% of potential drug candidates that are efficacious in preclinical tests are unsuccessful in clinical trials[33]. Better understanding of the organoid model and its recapitulation of the tumor microenvironment could provide valuable insight for potential drug screenings. Furthermore, current techniques for studying hypoxia result in exposing cells to normoxic and hypoxic conditions, which does not fully capture the oxygen gradient within the tumor. Therefore, there is a need for an experimental organoid model that can recapitulate tumor hypoxia to examine drug resistance and to study the effect of hypoxia on tumor progression and metastasis.

Although some studies have shown that there exists an oxygen gradient, not much is known about how oxygen diffuses through the 3D matrices[37,42]. Hypoxic cores have been studied in some spheroid models, but the extent of this core formation in cultures grown in normoxic conditions with the organoid model is poorly understood. The seeding density, time in culture, and scaffold material could influence the oxygen level within the overall gel as well as each organoid. It is important to consider how oxygen consumption could change over the course of an experiment and influence cell culture findings.

In our lab, we developed organoids from a triple transgenic hypoxia fate-mapping mouse model, which causes the permanent switch from TdTomato, a red fluorescent protein, to GFP, a green fluorescent protein. We investigated the hypoxic response of the organoids to determine the most sensitive mouse model and investigate the differences between organoids embedded in Matrigel and collagen. We also characterized the O_2 content of organoids in Matrigel and collagen and compare it to our hypoxia fate-mapping MDA-MB-231 spheroid model.

Chapter 2

Materials and Methods

2.1 Cell Culture

Human breast carcinoma cells, MDA-MB-231 (ATCC) were maintained in Dulbecco's modified Eagle's medium (DMEM) (Sigma-Aldrich) supplemented with 10% Fetal Bovine Serum (FBS, Corning) and 1% penicillin/streptomycin (Invitrogen). Cells were cultured in a humidified atmosphere at 37°C with 5% CO_2. Hypoxic cells were maintained inside a customized sealed chamber (McCoy) with a humidified atmosphere maintained at 37°C with 0.5% O_2, 5% CO_2, and 94.5% N_2.

2.2 Hypoxia Fate-mapping Cell Line

MDA-MB-231 breast cancer cells were transduced with two independent lentiviral vectors to generate a hypoxia fate-mapping cell line. The first lentiviral vector encodes CMV-loxp-DsRed-loxp-eGFP (Fig. 1). This vector contains a DsRed gene followed by a stop codon, which is flanked by two loxp sites, and in front of an eGFP gene (Fig. 1a). Under normal oxygen conditions, the cells express DsRed, a red fluorescent protein. The second lentiviral vector encodes 4xHRE-minTK-CRE-ODD that drive Cre production. Therefore, under hypoxia, the deletion of the DsRed gene occurs and eGFP, a green fluorescent protein, is permanently expressed. The cell line was single cell cloned and screened using image analysis and flow cytometry.

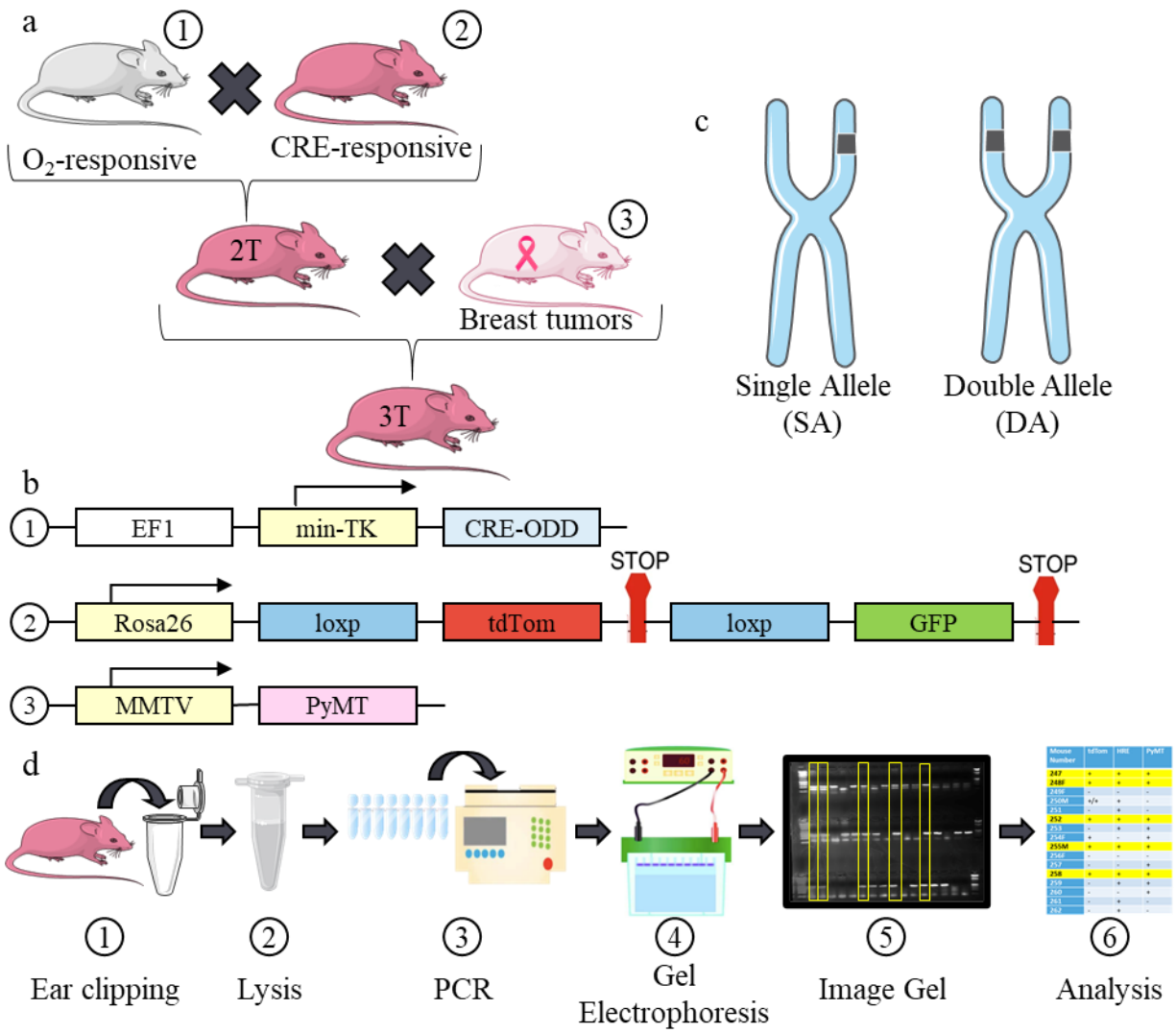

Figure 2: Hypoxia fate-mapping transgenic mouse model a. (1) The Gilkes lab generated a transgenic mouse that produces Cre recombinase in cells exposed to hypoxia. The hypoxia-inducible Cre mouse was crossed with a (2) mT/mG reporter mouse (B6.129(Cg)-Gt(ROSA)26Sor, Jackson Labs; 007676) to generate a double-transgenic (2T) mouse. The 2T mouse was bred with (3) a mouse that develops spontaneous breast tumors due to the expression of the PyMT oncogene that is driven by the mammary specific MMTV promoter. b. Transgene design of (1) the EF1-CRE-ODD gene integrated into the oxygen responsive mouse, (2) mT/mG reporter mouse, and (3) MMTV-PyMT expressing mouse. c. Transgenic genes are located on either one or both of the chromosomes. d. Schematic of the PCR assay used to identify mice that are positive for transgene integration. (1) Ear clippings of the 3T mice were (2) lysed to generate genomic DNA. (3) DNA was PCR amplified using the primers each transgene shown in b. The PCR product was separated using (4) gel electrophoresis. (5) The gel was imaged and (6) the mice with the genes of interest were maintained for further experimentation.

2.3 Hypoxia Fate-mapping Transgenic Mouse Model

The EF1-CRE-ODD sequence was inserted via pronuclear injection into mouse embryos. This oxygen responsive mouse was bred with tdTomato-floxed GFP (mT/mG) reporter mouse

(B6.129(Cg)-Gt(ROSA)26Sor, Jackson Labs, 007676) as shown in Figure 2. A female double transgenic hypoxia fate-mapping mouse was crossed with a male mouse that generates spontaneous breast tumors using the MMTV promoter driven PyMT oncogene (FVB/N-Tg(MMTV-PyMT), Jackson Labs, 002374). Female triple-transgenic mice are genotyped and kept for future experiments.

Upon sacrificing, the mammary fat pads (MFP) located on the right side of the mouse were removed, fixed with 4% PFA, and incubated at 4°C for 4 hours. Then, the tumors were placed in 30% sucrose (Sigma-Aldrich) and left at 4°C overnight. Next, the tumor tissue was embedded in OCT media (Fisher Scientific) and flash frozen using liquid nitrogen. The cryotome CM1100 (Leica) was used to generate tissue sections that were mounted onto Superfrost Plus Microscope Slides (Fisher Scientific). The tissue was stained with DAPI (1:1000) for 15 min at room temperature. Then, the slides were imaged using the RFP, GFP, and DAPI channels to evaluate the GFP and TdTom expression in the tissue. The samples were imaged using a Cytation 5 with an Olympus (LUCPLFLN 40XPh) phase objective (BioTek Instruments).

2.4 Genotyping

A PCR assay was used for the detection of transgenes as shown in Figure 2d. A clipping of the mouse's ear was lysed using lysis buffer (1M Tris pH 8.0, 5M NaCl, 0.5M EDTA, 10% Tween20, 10% NP-40 and ~40 µg of proteinase K). After being incubated overnight at 37°C with 5-minute interval shaking (1450 rpm), proteinase K was deactivated at 95°C for 2 minutes. Then, the genomic DNA was PCR amplified using primers for the 3 transgenes of interest (Table 1) and DreamTaq Green (Thermo Scientific) as follows: 95°C for 3 minutes, 40x (95°C for 30 seconds, 57°C for 35 seconds, 72°C for 35 seconds) and 72°C for 5 minutes. Next, gel electrophoresis was

performed using a 2% agarose gel. Images of the gel were captured using Azure eSeries Capture Program. Mice with the genes of interest were kept for further experimentation.

Sequence of interest	**FW**	**RV**
MMTV-PYMT	GGAAGCAAGTACTTCACAAGGG	GGAAAGTCACTAGGAGCAGGG
HRE	CTGCTAACCATGTTCATGCCTTC	GACGATGAAGCATGTTTAGCTGGC
TdTm – Mutant	CTT TAAGCCTGCCCAGAAGA	TAGAGCTTGCGGAACCCTTC
TdTm – WT	CTTTAAGCCTGCCCAGAAGA	AGGGAGCTGCAGTGGAGTAG

Table 1: Primer Sequences used for Genotyping

2.5 Organoid Culture

2.5.1 Organoid Processing

Mammary organoids were derived from transgenic mouse tumors following previously published protocols with minor modifications[38]. Tumors from the mammary fat pad of transgenic mice were mechanically disrupted using a blade. Then, the minced tumors were enzymatically digested in 2mg/mL of collagenase in Dulbecco's Modified Eagle's Medium/Ham's Nutrient Mixture F12 (DMEM/F12, Thermo Fisher) and incubated at 37°C for one hour on an orbital shaker at 180 rpm (Sigma-Aldrich). This suspension was centrifuged at 1500 x g for 10 minutes. The supernatant was discarded and the organoids were resuspended in fresh DMEM/F12 media. The suspension was centrifuged again at 1500 x g for 10 minutes and the supernatant was discarded. Organoids were digested with DNAse in a final concentration 0.1 mg/mL (Sigma-Aldrich) for 5 minutes at room temperature. This suspension was spun down for 10 minutes at

1500 x g. After resuspension in fresh media, the suspension was differentially centrifuged (4x) by pulsing to 1500 x g for 2 seconds. The isolated organoids were frozen for future experiments using 10% DMSO in Dulbecco's Modified Eagle's Medium/Ham's Nutrient Mixture F12 (DMEM/F12) supplemented with 1% Insulin-Transferrin-Selenium (ITS), 1% penicillin/streptomycin, and FGF (40 ng/mL) (Sigma-Aldrich).

2.5.2 Organoid Culture

Organoids were thawed, resuspended in fresh media, and centrifuged at 1500 x g for 10 minutes. The supernatant was discarded and the organoids were resuspended thoroughly in fresh media. Then, the total number of organoids were calculated by transferring 50 μL of the suspension to a petri dish and counting the number in a sample volume under a microscope. The desired number of organoids were embedded either in Matrigel (Corning) or soluble rat tail type I collagen (Corning) and 100 μL of gel were plated in the center of each well in a 24-well plate. For collagen embedment, the 24-well plate was heated on a heating block to 37°C for 20 minutes. Collagen was mixed with a 1:1 solution of DMEM/F12 cell medium and reconstitution buffer [0.2 HEPES (Sigma-Aldrich) and 0.26 M $NaHCO_3$ (Sigma-Aldrich) in water] to make a final concentration of 2mg/mL. NaOH (1 M) was added to neutralize the pH. After plating the organoids, the plates were incubated for 30 minutes at 5% CO_2 and 37°C. Next, 1 mL of warmed DMEM/F12 media supplemented with 1% ITS, 1% penicillin/streptomycin, and FGF (40 ng/mL) (Sigma-Aldrich) was added to each well. The media was refreshed in each well every 3-4 days.

Organoids are incubated under normal conditions overnight before being exposed to different oxygen levels. Different oxygen levels were achieved as follows: the InvivO2

workstation (Baker) with an ICONIC (Baker) electronically controlled gas-mixing system maintained at 37°C and equilibrated at 1% O_2, 5% CO_2, and 94% N_2, customized sealed chamber (McCoy) with a humidified atmosphere maintained at 37°C with 0.5% O_2, 5% CO_2, and 94.5% N_2 or 10% O_2, 5% CO_2, and 85% N_2, or in a modular chamber (Billups-Rothenberg) flushed with a gas mixture containing 5% O_2, 5% CO_2, and 90% N_2 maintained inside an incubator at 37°C.

2.5.3 Image Processing and Analysis

Organoids were imaged over time (day 1, 5, 10, and 20) by a Cytation 5 with an Olympus (PLAPON 1.25XPh) phase objective (BioTek Instruments) using the RFP and GFP channels. During imaging, the stage was incubated at 37°C. The entire well of the 24-well plate was captured using an X:Y montage and the image tiles were stitched using the Gen5 Software (Biotek). Cellular analysis was performed using the Gen5 software to segment objects and identify the size, circularity, mean RFP intensity, and mean GFP intensity of each organoid.

2.5.4 Flow Cytometry Analysis

Warm trypsin was added to each well and the gels were mechanically disrupted. The plate was incubated with trypsin for 10 minutes at 37°C. After being resuspended, they were centrifuged at 1500 x g for 5 minutes and washed twice with PBS. Then, the organoids were resuspended and collected in FACs buffer (PBS, 1% BSA, 0.5 mM EDTA, and 25 µg/ml DNAse). GFP was detected in the FITC channel and TdTom was detected in the PE channel using an SH800S Cell Sorter (Sony). Organoids created from a mouse with mT/mG and MMTV-PyMT (2T) transgenes

were used as a TdTom+/GFP- control. Then, flow cytometry analysis was performed FlowJo V10 software (Tree Star, Inc.).

2.6 Confocal Microscopy

Confocal microscopy was performed on the organoid cultures to visualize individual organoids. Wells of a 24-well glass bottom microplate were coated with soluble rat tail type I collagen (Corning) in acetic acid (final concentration 50 mg/mL). The plate was incubated at room temperature for 1 hour and, then, washed 3X with PBS. Organoids were plated as previously described. Confocal microscopy was performed to obtain z projections of organoids using a 20X/0.80 PlanApo (dry, no DIC) objective and 40×/1.30 PlanNeofluar oil objective in a Zeiss LSM780-FCS microscope. The z-stacks were processed via ZEN imaging software (Zeiss).

2.7 Oxygen Monitoring Experiments

To correlate organoid number with oxygen concentration, different numbers of organoids were seeded into 24-well plates. Oxygen measurements were conducted using a REDFLASH system (FireStingO2, Pyroscience). OXNANO oxygen nanoprobes were dispersed in Matrigel and collagen gels during cell plating. Oxygen levels were measured through the bottom of the well once daily using the REDFLASH oxygen meter. The sensor was calibrated daily using nanoprobes suspended in water.

2.8 Spheroid Culture

Hypoxia fate-mapping MDA-MB-231 cells were counted and dispersed in Matrigel and 100 µL were placed in the center of the well of a 24-well plate. Then, the spheroids were incubated at

37°C for 30 minutes. Next, warmed DMEM media supplemented with 10% FBS and 1% penicillin/streptomycin was added to each well. The spheroids were maintained in a humidified environment at 37°C and 5% CO_2. Then, the plate was imaged in a Cytation 5 using an Olympus (PLAPON 1.25XPh) phase objective (BioTek Instruments).

2.9 Statistical Analysis

The mean values ± standard error of mean (SEM) were calculated and plotted using Graphpad Prism 6 software (GraphPad Software, Inc.). One-way and two-way ANOVA and t-tests were used to determine significance, indicated in graphs using ****P < 0.0001, ***P < 0.001, **P < 0.01, *P < 0.1.

Chapter 3

Results and Discussion

3.1 Establishing a Hypoxia Fate-mapping Organoid Model

A hypoxia fate-mapping triple transgenic mouse system was recently developed in the Gilkes laboratory[29] . A mouse engineered to express Cre enzyme in cells at low levels of O_2 was designed by introducing the EF1-CREODD transgene via pronuclear injection into mouse embryos. The EF1-CREODD mouse was crossed with a tdTomato-floxed GFP (mT/mG) reporter mouse that triggers a switch from TdTomato to GFP expression in the presence of Cre. Then, female double-transgenic mice were crossed with the FVB/N-Tg(MMTV-PyMT) male mice, which develops spontaneous breast cancer (Fig. 2a,b). The female triple-transgenic mice develop mammary tumors, in which cancer cells switch from TdTomato to permanent GFP expression upon exposure to hypoxia. To evaluate the best combination of allele number of the EF1-CREODD and TdTm transgenes in terms of sensitivity to hypoxia, we utilized an organoid model and performed studies *in vitro*. First, genotyping was performed to identify mice with either EF1-CREODD(+/+)TdTm(+/+), EF1-CREODD(+/-)TdTm(+/+), EF1-CREODD(+/-)TdTm(+/-), or TdTm(+/+), (Fig. 2c,d). Then, organoids were generated from the mammary tumors that developed in triple transgenic mice (Fig. 2a). The organoids were cultured at various O_2 concentrations depending upon the experiment.

3.1.1 Determining the Role of TdTm Allele Number

PyMT tumors from mice expressing either a single- or double-allele of TdTm transgenes were tested: EF1-CREODD(+/-)TdTm(+/+) and EF1-CREODD(+/-)TdTm(+/-). Organoids from each

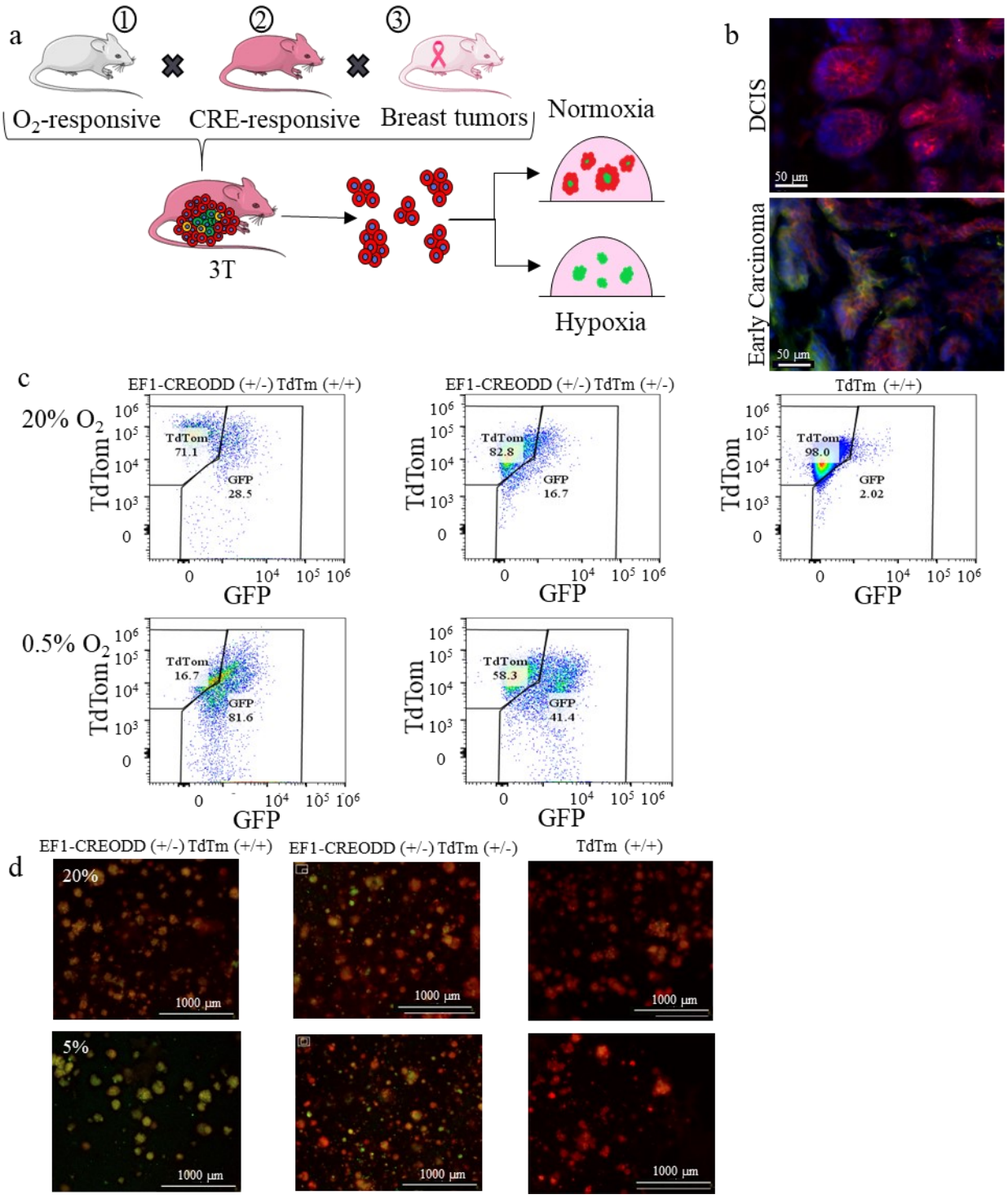

Figure 3: Tumor organoids with single- and double-allele of the TdTm transgene a. Tumors from the hypoxia-responsive triple-transgenic mice were used to generate organoids. The organoids were embedded into Matrigel. The organoids were cultured under hypoxic and normoxic conditions. b. Fluorescent images of frozen tissue sections of 3T mouse tumor showing ductal carcinoma in situ (DCIS) and early carcinoma. c. Representative plots of flow cytometry data from organoids from EF1-CREODD(+/-)TdTm(+/+), EF1-CREODD(+/-)TdTm(+/-), and TdTm(+/+) mice embedded in Matrigel and cultured under 20% or 0.5% O_2 for 20 days. d. Fluorescent images of tumor organoids embedded in Matrigel following 20 days of exposure to 20% and 5% O_2.

mouse tumor were embedded in Matrigel and cultured at 20%, 5%, and 0.5% O_2 for 20 days. Fluorescent microscopy and flow cytometry were used to assess the levels of TdTomato and GFP expression. Double transgenic mice, without the O_2-responsive vector, were used as a control determine the background levels of GFP expression for both imaging and flow cytometry. EF1-CREODD(+/-)TdTm(+/+) organoids contained 2-fold more GFP+ cells than EF1-CREODD(+/-)TdTm(+/-) when exposed to 0.5% (Fig. 3c). For EF1-CREODD(+/-)TdTm(+/+) and EF1-CREODD(+/-)TdTm(+/-), larger organoids cultured at 20% O_2 showed GFP+ expression located within the center of the organoid (Fig 3d). The organoids cultured under 5% visually appeared more GFP+ than the 20% organoids. To summarize, organoids derived from mice with two alleles of the TdTm transgene contained more GFP+ cells under 0.5% O_2 than the single allele TdTm organoids (Fig. 3 c,d).

3.1.2 Determining the Role of EF1-CREODD Allele Number

To determine if the copy number of the EF1-CREODD transgene affects sensitivity to hypoxia, organoids derived from EF1-CREODD(+/+)TdTm(+/+), EF1-CREODD(+/-)TdTm(+/+), and TdTm(+/+) mice were plated in Matrigel and exposed to 20% and 0.5% O_2 for 20 days. On day 20, organoids were analyzed for GFP and TdTom expression by flow cytometry (Fig. 4a). No significant difference in the number of GFP+ expressing cells was detected in the single- versus double-allele EF1-CREODD organoids (Fig. 4b,c). Organoids were also plated and exposed to 20% and 5% O_2 and no notable difference was detected between the EF1-CREODD(+/+)TdTm(+/+) and EF1-CREODD(+/-)TdTm(+/+) (Fig. 4d). Under 5% O_2 conditions, GFP+ cells were localized in the center of the organoid similar to organoids cultured under 20% O_2 conditions, but with visually brighter GFP cores. We expected a second allele of

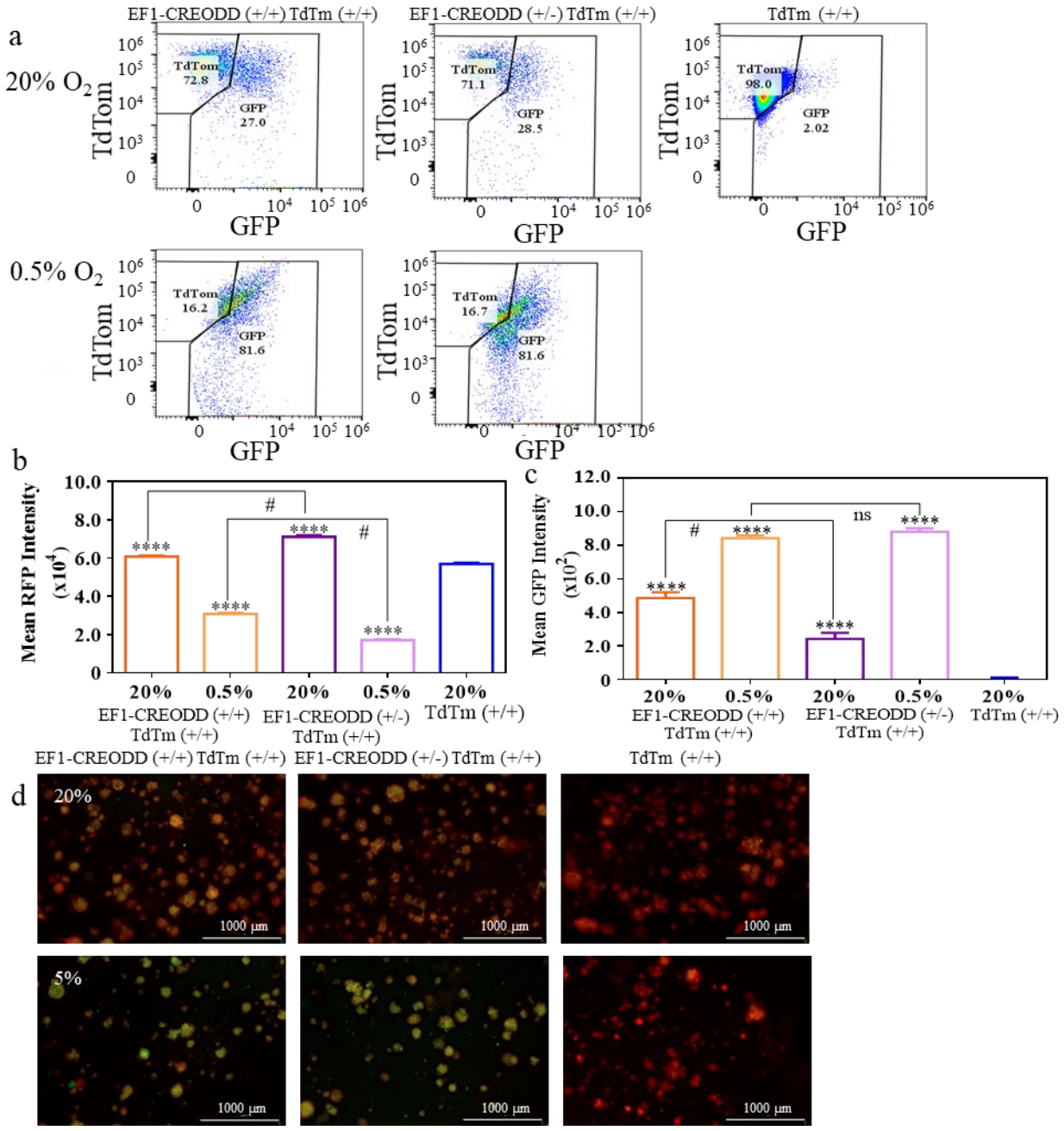

Figure 4: Tumor organoids with single- and double-allele of the EF1-CREODD transgene a. Representative plots of flow cytometry data for organoids exposed to 20% and 0.5 % O_2 for 20 days. b. Mean RFP intensity for flow cytometry of organoids exposed to 20% and 0.5% for 20 days (mean ± SEM, N = 1, n = 7000); ****P < 0.0001 versus 20% TdTm(+/+) (one-way ANOVA); ####P<0.0001 (t-test). c. Mean GFP intensity for flow cytometry of organoids exposed to 20% and 0.5% for 20 days (mean ± SEM, N = 1, n = 6000); ****P < 0.0001 versus 20% TdTm(+/+) (one-way ANOVA); ####P<0.0001 (t-test). d. Fluorescent images of organoids from the triple-transgenic mice following 20 days of exposure to 20% and 5% O_2.

EF1-CREODD to enhance sensitivity; however, taken together the results suggest that introducing a second allele of the EF1-CREODD transgene does not enhance sensitivity to hypoxia. Therefore, the EF1-CREODD (+/-) TdTm (+/+) was used for future experiments.

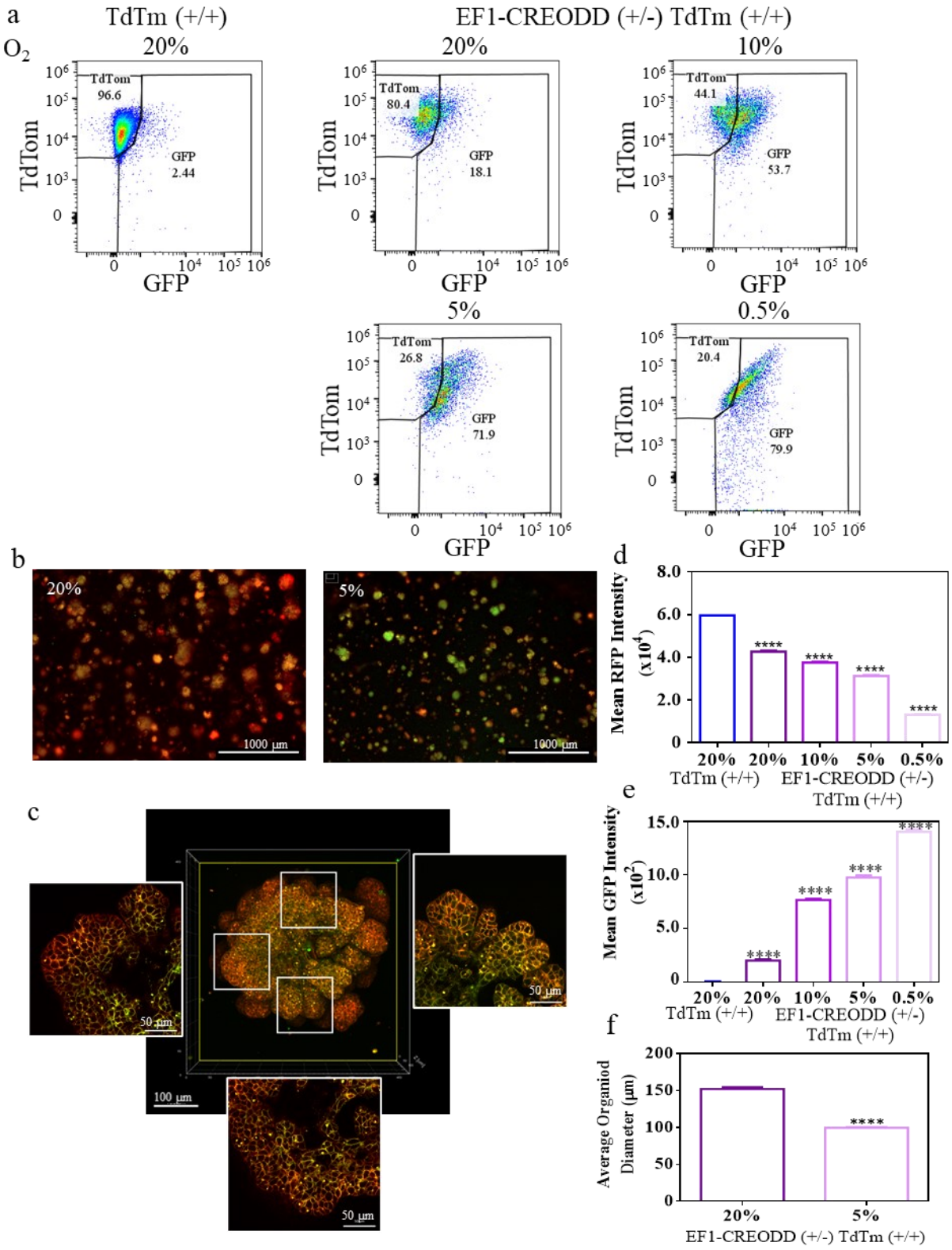

Figure 5: EF1-CREODD(+/-)TdTm(+/+) tumor organoids at different O_2 levels a. Representative plots of flow cytometry data for EF1-CREODD(+/-)TdTm(+/+) and TdTm(+/+) organoids exposed to 20%, 10%, 5%, and 0.5% O_2 for 20 days. b. Fluorescent images of EF1-CREODD(+/-)TdTm(+/+) organoids exposed to 20% and 5% O_2 for

20 days. c. Fluorescent images of EF1-CREODD(+/-)TdTm(+/+) organoids after 11 days. d. Mean RFP intensity for flow cytometry of organoids exposed to 20%, 10%, and 5% for 20 days (mean ± SEM, N = 1, n = 5000-8000); ****P < 0.0001 versus 20% TdTm(+/+) (one-way ANOVA). e. Mean GFP intensity for flow cytometry of organoids exposed to 20%, 10%, and 5% for 20 days (mean ± SEM, N = 1, n = 5000-8000); ****P < 0.0001 versus 20% TdTm(+/+) (one-way ANOVA). f. Average organoid size using image analysis, corresponding to fluorescent images (b) (mean ± SEM, N = 1, n = 1000-2000); ****P < 0.0001 (t-test).

3.2 Effect of Different O_2 Levels in Hypoxia Fate-mapping Organoids

Organoids were cultured under different O_2 concentrations (20%, 10%, 5% and 0.5% O_2) to determine the effect of O_2 concentration on our hypoxia fate-mapping system. After 20 days of culture in Matrigel, the organoids derived from the mammary tumors of EF1-CREODD(+/-)TdTm(+/+) were collected for flow cytometry analysis (Fig. 5a). Organoids cultured under 20% O_2 showed a GFP+ core as described previously (Fig. 5b,c). Under 5% O_2, most of the organoids appeared to have higher GFP expression in the cores and some of the organoids became completely GFP+ (Fig. 5b). The mean TdTom intensity decreased with lower O_2 concentrations, whereas the mean GFP intensity increased as measured by flow cytometry analysis (Fig. 5d,e). Organoids exposed to 10%, 5%, and 0.5% O_2 had 3.8X, 4.9X, and 6.9X higher levels of GFP expression, respectively, compared to those cultured under 20% O_2. This indicated an inverse correlation between O_2 level and GFP intensity. Interestingly, we observed that organoids showed slower growth under 5% when compared to 20% (Fig. 5f).

3.3 Effect of Matrix Type in Hypoxia Fate-mapping Organoids

Given that organoids cultured in Matrigel under 20% O_2 conditions have GFP+ cores after long-term culture, we sought to investigate this occurrence in collagen matrices. The collagen matrix promotes an invasive phenotype that has been previously described[38], therefore, the organoids in collagen became less circular, more elongated, and invaded into the surrounding matrix (Fig.

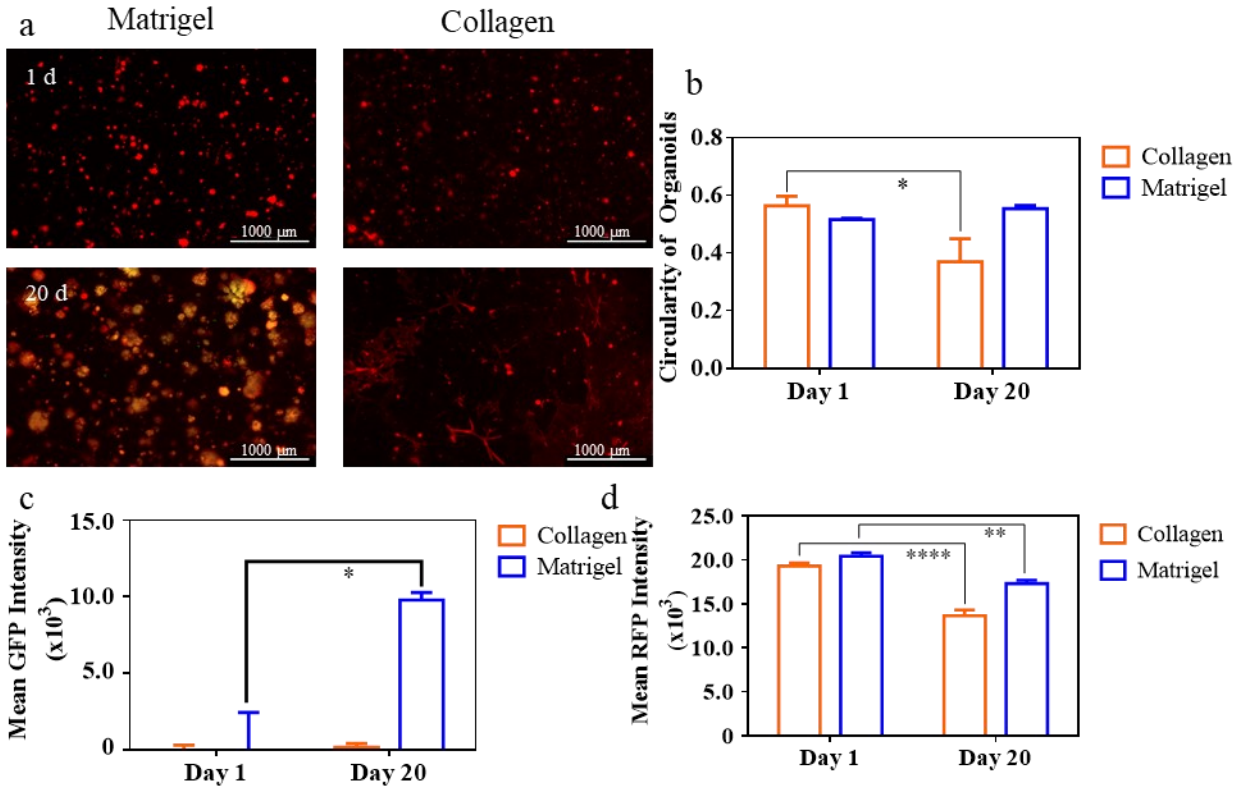

Figure 6: EF1-CREODD(+/-)TdTm(+/+) tumor organoids embedded in Matrigel and collagen
a. Fluorescent images of EF1-CREODD(+/-)TdTm(+/+) organoids cultured in Matrigel and collagen gels under 20% oxygen for 20 days. b. Circularity of organoids in 3D matrices for 20 days (mean ± SEM, N = 1, n = 1000-2000); ****P<0.0001 (t-test). c. Image analysis of fluorescent images (a) was used to calculate average GFP intensity for organoids grown in 3D matrices for 20 days (mean ± SEM, N = 1, n = 1000-2000) ****P<0.0001 (t-test). d. Image analysis of fluorescent images (a) was used to calculate average RFP intensity for organoids grown in 3D matrices for 20 days (mean ± SEM, N = 1, n = 1000-2000) ****P<0.0001 (t-test).

6a,b). While the GFP mean intensity increased in Matrigel, it was unchanged in a collagen matrix (Fig. 6c,d).

3.4 Effect of Organoid Density on O_2 Distributions in Matrices

Given that the change in O_2 levels over time could be a significant environmental cue that determines the fate of individual cells within organoids cultured in 3D matrices[29], we wanted to characterize the O_2 concentration in Matrigel and collagen matrices. Organoids were plated in both Matrigel and collagen and OXNANO nanoprobes were dispersed throughout the matrices. The nanoprobe signal was read through the bottom of the wells containing the organoid matrices

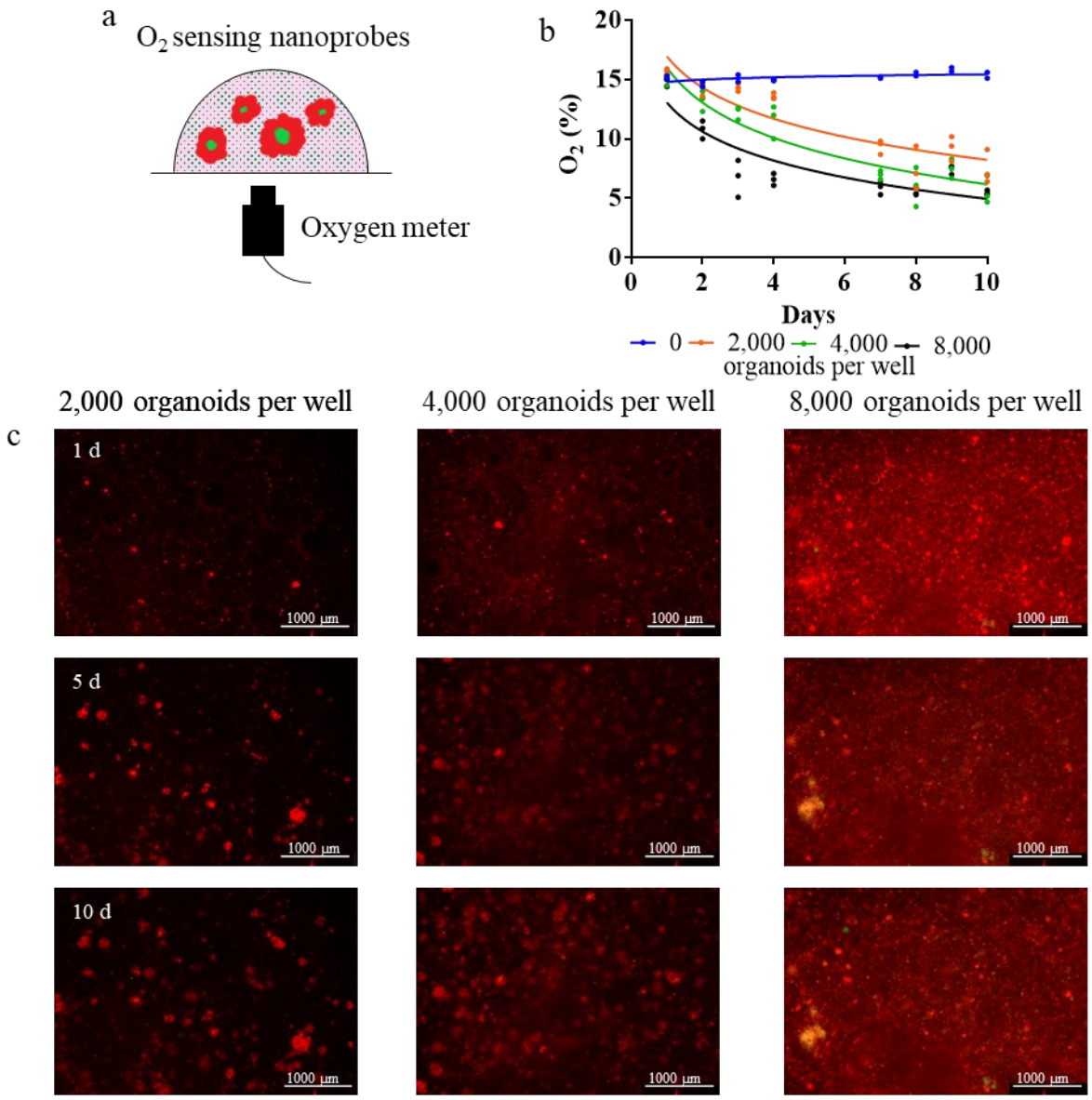

Figure 7: Tumor organoids embedded in Matrigel with OXNANO nanoprobes a. OXNANO nanoprobes were suspended in 3D matrices. b. Oxygen was measured for EF1-CREODD(+/-)TdTm(+/+) organoids cultured in Matrigel. Organoids were seeded at 2,000, 4,000, and 8,000 organoids per well (mean ± SEM, N = 1, n = 3). c. Time course fluorescent images of organoids in Matrigel.

(Fig. 7a). Nanoprobes were also added to collagen and Matrigel matrices without organoids as a background control. The O_2 concentration in the empty wells was approximately 15%. Over 10 days in culture, the O_2 levels in Matrigel decreased from 15% to under 6% in wells with an initial density of 8,000 organoids per well. A higher initial density of organoids caused greater decreases in O_2 levels observed overtime (Fig. 7b,c). In summary, the initial number of

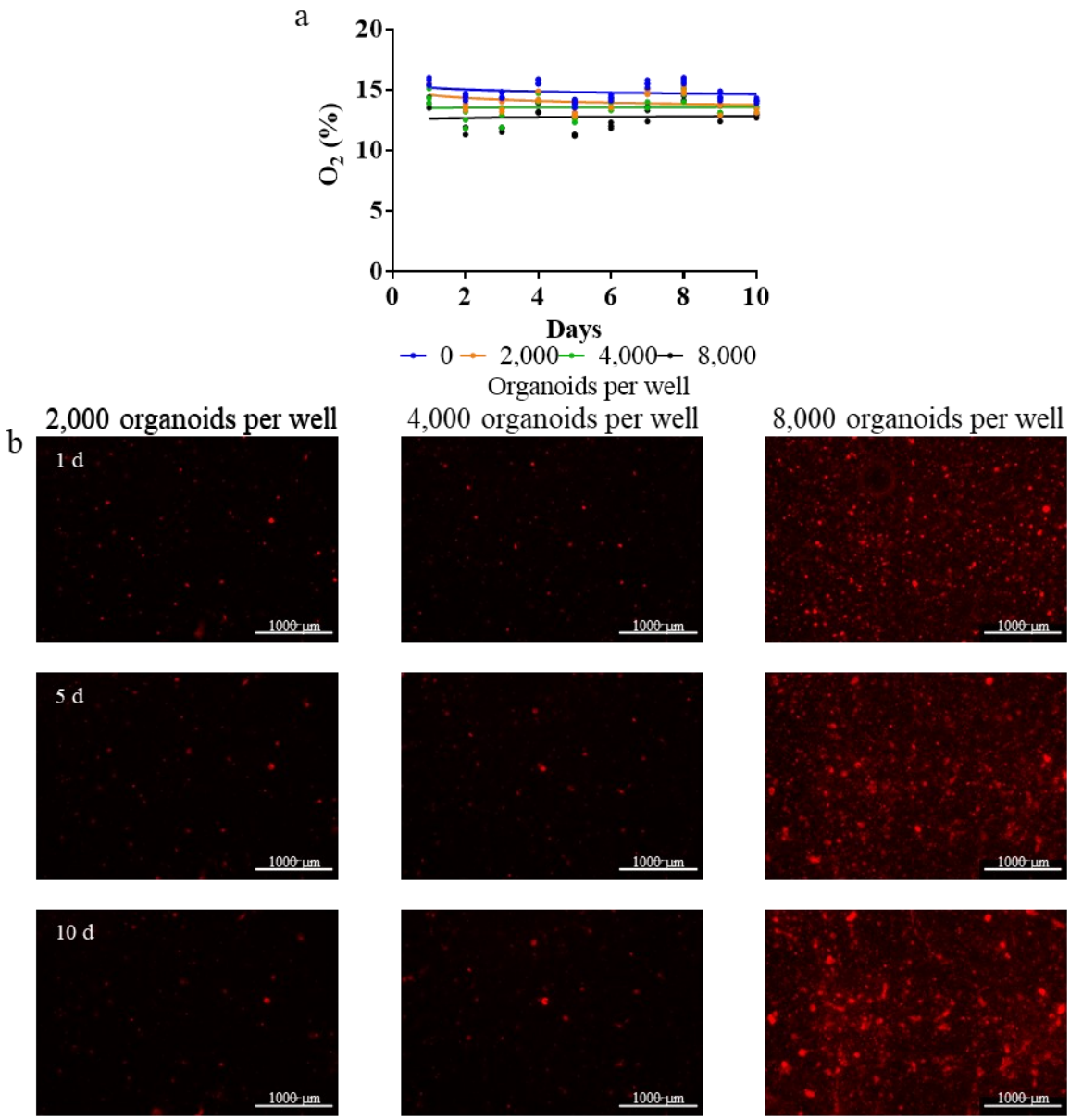

Figure 8: Tumor organoids embedded in collagen with OXNANO nanoprobes a. Oxygen was measured with OXNANO nanoprobes for EF1-CREODD(+/-)TdTm(+/+) organoids cultured in a collagen gel. Organoids were seeded at 2,000, 4,000, and 8,000 organoids per well (mean ± SEM, N = 1, n = 3). c. Time course fluorescent images of organoids in a collagen gel.

organoids plated may cause a decrease in O_2 over time and lead to hypoxic cores in Matrigel matrices.

We performed a similar study in collagen matrices and detected no change in O_2 levels over time (Fig. 8a). The organoids appear to invade into the surrounding collagen matrix over

time (Fig. 8b). Thus, the O_2 content decreased in Matrigel with increasing density, but was unaffected for organoids embedded in collagen.

3.5 Effect of MDA-MB-231 Spheroid Density on O_2 Distribution in Matrigel

The hypoxia fate-mapping system was first created using a cell line, as previously described. MDA-MD-231 cells were transfected with the two vectors to drive Cre expression under hypoxia and trigger a fluorescent switch from DsRed to GFP (Fig. 1). These cells were single cell cloned to ensure they were consistently responsive to 0.5% O_2, but not to 3% O_2 in terms of GFP activation. In order to further explore our results revealing a hypoxic GFP+ core in organoids cultured in Matrigel under 20% O_2 conditions, we used the MDA-MB-231 hypoxia fate-mapping cell line to generate spheroids in the same conditions. Single cells were seed in Matrigel to create spheroids and OXNANO nanoprobes were dispersed throughout the matrix. Over time, the O_2 levels decreased significantly in the wells with spheroids (Fig. 9a,b). Notably, higher cell seeding caused greater O_2 decrease over time. At day 10, these hypoxia fate-mapping spheroids developed GFP+ cores indicating that the cores of these spheroids experience hypoxic conditions when cultured at 20% O_2 for 10 days. However, the O_2 level of the MDA-MB-231 spheroids is higher than the one registered for 3T tumor organoids at day 10. This could be due to the decreased oxygen consumption rate in the MDA-MB-231 system. It was reported that MDA-MB-231 cells have an oxygen consumption rate of 16.8 amol $s^{-1}cell^{-1}$, while mouse carcinoma cells have a rate of 27 amol $s^{-1}cell^{-1}$, which could lead to less oxygen being consumed by the MDA-MB-231 spheroids[43]. These spheroids reached larger dimensions at day 10 than organoids so higher proliferation is likely related to a more drastic formation of a hypoxic core and activation of GFP expression.

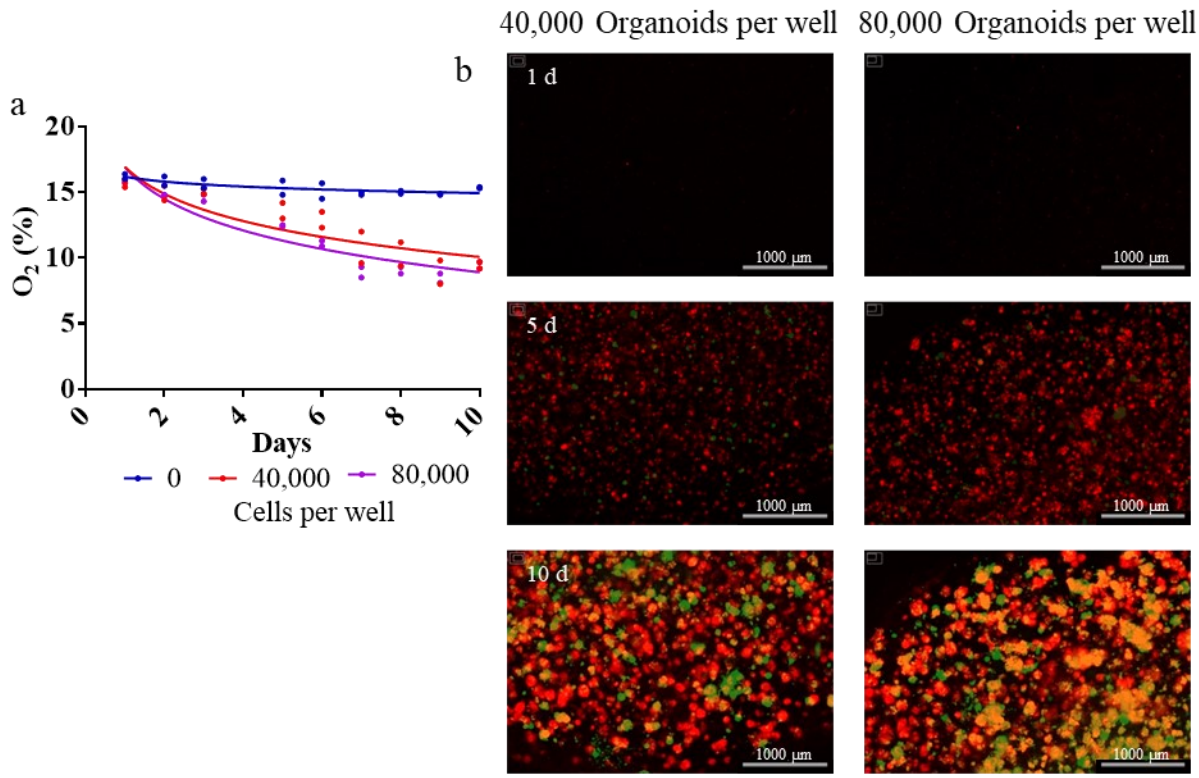

Figure 9: MDA-MB-231 hypoxia fate-mapping cells embedded in Matrigel with OXNANO nanoprobes
a. Oxygen was measured with OXNANO nanoprobes for MDA-MB-231 spheroids with the hypoxia fate-mapping system cultured in Matrigel. Cells were seeded at 40,000 and 80,000 cells per well (mean ± SEM, N = 1, n =2). b. Time course fluorescent images of organoids in Matrigel.

3.6 Discussion

Recent developments in 3D culture systems facilitate better recapitulation of the tumor microenvironment and allow for long-term culture[44–46]. Besides capturing the 3D structure, there is still more to be uncovered about how organoids mimic the tumor microenvironment. For instance, current studies indicate the behavior of cancer cells depends on the properties of the extracellular matrix and the diffusion of nutrients through it[41,47,48]. Oxygen distribution is a crucial factor in the tumor microenvironment and understanding how individual organoids experience this effect will determine how long-term culturing affects the characteristics of the organoids over time. Here, we utilized a hypoxia fate-mapping mouse model and OXNANO nanoprobes to investigate the overall O_2 content of tumor organoids. First, we wanted to find the

most sensitive mouse model to conduct our future experiments. In our triple transgenic mouse model, the EF1-CREODD transgene expresses Cre, which activates the cleavage of TdTomato from the TdTm transgene, causing cells to permanently express GFP. We hypothesized that changing the copy number of our TdTm transgenes could affect the fluorescent signal under hypoxia. The double allele for the reporter transgene (TdTm) increased the sensitivity of the organoids when exposed to 0.5% O_2 when compared to a single allele system (Fig. 3). Additionally, we expected that a double allele of the EF1-CREODD transgene would also affect the sensitivity due to increased Cre production. Markedly, no notable difference was detected between the double allele and the single allele of the EF1-CREODD transgene (Fig. 4). This is somewhat unexpected and we speculate that either more Cre is not being produced with a second allele or one allele creates enough Cre to saturate the system. Further studies would need to be conducted to determine which is the case. Taken together, the EF1-CREODD(+/-)TdTm(+/+) mouse was chosen to be used for future studies.

Next, we wanted to examine the effect of O_2 concentration on our hypoxia fate-mapping organoids. They were embedded in Matrigel and cultured under different O_2 concentrations (20%, 10%, 5% and 0.5% O_2). As the oxygen decreased, the organoids became more GFP+, and, thus, more hypoxic. Interestingly, at 20% O_2, the development of a hypoxic core was observed (Fig 5). Additionally, at 5% O_2, some of the organoids become completely GFP+ possibly indicating that the gel containing the organoids could have a lower O_2 content than 5%. Although it is known that organoids can develop hypoxic cores, very little is known about these cores and how they develop[42,45,49]. For an organoid cultured at 20% O_2 for 20 days, GFP+ cells appear to be localized in the center with the TdTm+ cells lining the edge (Fig. 5). Previous studies found

that the cell proliferation depends on location and proliferation is higher for cells on the organoid rim[30,45].

Interestingly, we found that the average diameter of the organoids decreased from 20% to 5% O_2. In previous studies, it was found that hypoxia contributed to slower proliferation and growth[5,50,51]. We hypothesize that organoids under lower O_2 are less proliferative and form smaller organoids. However, there is some evidence that shows low oxygen could enhance proliferation[23,52]. More studies investigating the difference between organoids at different oxygen levels would need to be conducted.

Next, since hypoxic cores formed in organoids embedded in Matrigel after long term culture, we explored the commonly used collagen I matrix to evaluate how hypoxic cores develop in this system. We found that organoids after 20 days in collagen had an invasive morphology and, therefore, did not form compact cores like observed in Matrigel (Fig. 6). Thus, while the GFP mean intensity increased in Matrigel, it did not change in a collagen matrix. In Matrigel, the organoids form large compact 3D structures, while in collagen the organoids spread out and elongate in several lengthy branches. The collagen matrix promotes an invasive phenotype that has been previously described[38,38,53], We hypothesize that the failure of organoids to grow in 3D compact spheres results in them to not developing hypoxic GFP+ cores over this time period. Perhaps increasing the culturing time for organoids embedded in Matrigel could lead to more compact structures and GFP+ signal in our system.

There are several key determining factors for why these hypoxic cores could be forming: cell density, scaffold material, and cell activity. First, we wanted to see how initial organoid seeding density would affect the oxygen distribution in Matrigel, since cell density has been shown to affect the degree of oxygen depletion in previous studies[52]. First, we confirmed that the

organoids grew and proliferated throughout the experiment. Organoids plated in Matrigel showed that higher organoid initial seeding caused greater decreases in O_2 levels observed overtime (Fig. 7). Additionally, the O_2 levels decreased sharply initially and then seemed to begin to plateau over time. This could be due to the shift in metabolic activity of the organoids as the more hypoxic cores shift from aerobic to anaerobic metabolism. More studies would need to be done to confirm this hypothesis. Decreasing O_2 levels resulted in hypoxic cores in compact spherical organoids in Matrigel.

Since hypoxic cores do not form in collagen over 20 days in culture, we hypothesized the oxygen distribution would not be affected in the more permeable collagen matrix[52]. We performed a similar study in collagen matrices by increasing organoid seeding density. We observed that although the organoids grow and proliferate throughout the experiment, initial number of organoids plated per well did not greatly affect O_2 level. We hypothesize that these organoids do not develop a GFP+ core due to a more invasive phenotype in collagen that decreases the ability of cells to compact or the high permeability of collagen to O_2.

We also investigated the O_2 depletion in hypoxia fate-mapping MDA-MB-231 derived spheroids in Matrigel. Higher cell seeding caused greater O_2 decrease over time. Interestingly, although GFP+ cores were detected in this model, the O_2 curves showed a less drastic depletion of O_2. A previous study found that the MDA-MB-231 cells consumed oxygen at a rate of 16.8 amol s^{-1} $cell^{-1}$, while mouse carcinoma cells had a rate of is 27 amol s^{-1} $cell^{-1}$.[43] This could prevent the MDA-MB-231 spheroids from reaching as low O_2 level as triple transgenic mouse tumor organoids. However, these spheroids reached larger dimensions at day 10 than organoids so higher proliferation is likely related to a more drastic formation of a hypoxic core and activation of GFP expression.

Our results can be utilized to design optimal conditions for 3D culture of breast cancer organoids. In conclusion, Matrigel is a better platform to study growth and spontaneous hypoxia, while collagen is a better matrix to investigate invasion. The 3D hypoxic environment allows for the study of hypoxic-nonhypoxic cell interactions. Therefore, developing consistent hypoxic cores could lead to a better understanding of tumor hypoxia, which could ultimately lead to drug and treatment development.

Chapter 4

Conclusion and Future Work

4.1 Conclusion

In this work, we investigated how O_2 content affected a hypoxia fate-mapping organoid model. We found the most sensitive mouse model through organoid culture had a single allele of the oxygen sensing EF1-CREODD transgene and two alleles of the Cre-responsive TdTm transgene. Then, we exposed EF1-CREODD(+/-)TdTm(+/+) organoids to various oxygen levels to define the hypoxic sensing ability of the organoids. An inverse relationship between GFP+ cells and O_2 level was found. We, also discovered when culturing organoids at 20% O_2, they develop GFP+ hypoxic cores after 20 days when embedded in Matrigel. However, when embedded in collagen, the organoids failed to generate hypoxic cores.

Furthermore, we monitored the O_2 level in Matrigel and collagen over time using OXNANO nanoprobes. With increasing initial organoid seeding density, the O_2 level decreased when embedded in Matrigel, but remained constant when embedded in collagen. This leads us to believe that the compact spherical structures formed in Matrigel allow for hypoxic core formation, while the invasive phenotype in collagen prevents it. Organoid culture in Matrigel may therefore be essential to recapitulate spontaneous hypoxic environments *in vitro*. Additionally, we used hypoxic fate-mapping MDA-MB-231 spheroids to monitor the oxygen distribution over time. We found similar results when embedded in Matrigel, which showed increasing initial cell seeding density leading to O_2 depletion. This work warrants additional studies into the hypoxic core formation of organoids in Matrigel to develop an innovative 3D

tumor model that can better recreate the tumor niches under well-defined and reproducible conditions.

4.2 Future Work

Future research to further characterize the formation of the hypoxic cores in the organoid system is required. We could generate mixtures of Matrigel and collagen in attempts to produce an invasive model, which develops hypoxic cores to determine the role of hypoxic cells in invasion. It was found that a mixture of collagen and Matrigel represents more physiological ECM microenvironments for breast tissue[38]. Hence, this could lead to a better understanding of the mechanism of invasion.

It would be interesting to utilize PrestoBlue and/or cell counting at each time point to determine the number of cells and their role in oxygen depletion. With the availability of nutrients becoming a concern in long-term 3D culture, we would like to model the oxygen transport in an organoid and spheroid using Michealis-Menten kinetics to further characterize the extent of the hypoxic cores. Additionally, we could develop cell lines from the hypoxia fate-mapping mouse models to generate spheroids and determine whether the difference in oxygen consumption rate of human MDA-MB-231 cells and mouse carcinoma cells explains our observation. By using, flow cytometry to sort GFP+ and TdTom+ cells isolated from organoids, we could examine the differences between hypoxic/post hypoxic and oxygenated cells. For instance, we could characterize these differences both at the RNA and the phenotypic level.

Additional studies about how hypoxic cores affect long term cultures are warranted since passaging of organoids can allow cultures to be maintained for months to years[44–46]. Given our observations, it is important to evaluate the possibility of spontaneous hypoxia in these systems

and determine whether hypoxic/post-hypoxic cells behave differently after several passages. Our fate mapping system could also provide insight into the origin of these cores. For instance, it could determine if the cores are a direct result of size or if they are influenced by other factors, such as matrix permeability, proximity to other organoids, or metabolic activity of specific cells. Lastly, we could use this high throughput organoid model with defined hypoxia for drug testing and development. This would be particularly useful since hypoxia has been largely implicated in chemoresistance[5].

Bibliography

1. American Cancer Society. *Cancer Facts & Figures 2020.* (American Cancer Society, 2020).
2. Gilkes, D. M., Semenza, G. L. & Wirtz, D. Hypoxia and the extracellular matrix: drivers of tumour metastasis. *Nature Reviews Cancer* **14**, 430 (2014).
3. Michiels, C. Physiological and Pathological Responses to Hypoxia. *The American Journal of Pathology* **164**, 1875–1882 (2004).
4. Wirtz, D., Konstantopoulos, K. & Searson, P. C. The physics of cancer: the role of physical interactions and mechanical forces in metastasis. *Nature Reviews Cancer* **11**, 512–522 (2011).
5. Cosse, J.-P. & Michiels, C. Tumour Hypoxia Affects the Responsiveness of Cancer Cells to Chemotherapy and Promotes Cancer Progression. *Anti-cancer agents in medicinal chemistry* **8**, 790–7 (2008).
6. Eales, K. L., Hollinshead, K. E. R. & Tennant, D. A. Hypoxia and metabolic adaptation of cancer cells. *Oncogenesis* **5**, e190 (2016).
7. Vaupel, P., Mayer, A. & Höckel, M. Tumor hypoxia and malignant progression. *Methods Enzymol* **381**, 335–354 (2004).
8. Semenza, G. L. HIF-1: mediator of physiological and pathophysiological responses to hypoxia. *Journal of Applied Physiology* **88**, 1474–1480 (2000).
9. Knowles, H. J. & Harris, A. L. Hypoxia and oxidative stress in breast cancer. Hypoxia and tumourigenesis. *Breast Cancer Res* **3**, 318–322 (2001).
10. Kim, J., Gao, P. & Dang, C. V. Effects of hypoxia on tumor metabolism. *Cancer and Metastasis Reviews* **26**, 291–298 (2007).

11. Jiang, B. H., Semenza, G. L., Bauer, C. & Marti, H. H. Hypoxia-inducible factor 1 levels vary exponentially over a physiologically relevant range of O2 tension. *American Journal of Physiology-Cell Physiology* **271**, C1172–C1180 (1996).
12. Szot, C. S., Buchanan, C. F., Freeman, J. W. & Rylander, M. N. 3D in vitro bioengineered tumors based on collagen I hydrogels. *Biomaterials* **32**, 7905–7912 (2011).
13. Semenza, G. L. Hypoxia-inducible factors: mediators of cancer progression and targets for cancer therapy. *Trends Pharmacol Sci* **33**, 207–214 (2012).
14. Rademakers, S. E., Lok, J., van der Kogel, A. J., Bussink, J. & Kaanders, J. H. Metabolic markers in relation to hypoxia; staining patterns and colocalization of pimonidazole, HIF-1α, CAIX, LDH-5, GLUT-1, MCT1 and MCT4. *BMC Cancer* **11**, 167 (2011).
15. Muz, B., de la Puente, P., Azab, F. & Azab, A. K. The role of hypoxia in cancer progression, angiogenesis, metastasis, and resistance to therapy. *Hypoxia (Auckl)* **3**, 83–92 (2015).
16. Nagelkerke, A. *et al.* Hypoxia stimulates migration of breast cancer cells via the PERK/ATF4/LAMP3-arm of the unfolded protein response. *Breast Cancer Research* **15**, R2 (2013).
17. Liu, Z.-J., Semenza, G. L. & Zhang, H.-F. Hypoxia-inducible factor 1 and breast cancer metastasis. *J Zhejiang Univ Sci B* **16**, 32–43 (2015).
18. Vaupel, P., Höckel, M. & Mayer, A. Detection and characterization of tumor hypoxia using pO2 histography. *Antioxid Redox Signal* **9**, 1221–1235 (2007).
19. Zhang, H. *et al.* HIF-1-dependent expression of angiopoietin-like 4 and L1CAM mediates vascular metastasis of hypoxic breast cancer cells to the lungs. *Oncogene* **31**, 1757–1770 (2012).

20. Rankin, E. B. & Giaccia, A. J. The role of hypoxia-inducible factors in tumorigenesis. *Cell Death Differ* **15**, 678–685 (2008).
21. Ye, I. C. *et al.* Molecular Portrait of Hypoxia in Breast Cancer: A Prognostic Signature and Novel. *Mol Cancer Res* **16**, 1889–1901 (2018).
22. Semenza, G. L. HIF-1 and human disease: one highly involved factor. *Genes Dev* **14**, 1983–1991 (2000).
23. Jun, J. C., Rathore, A., Younas, H., Gilkes, D. & Polotsky, V. Y. Hypoxia-Inducible Factors and Cancer. *Curr Sleep Med Rep* **3**, 1–10 (2017).
24. Lu, X. & Kang, Y. Hypoxia and hypoxia-inducible factors: master regulators of metastasis. *Clin Cancer Res* **16**, 5928–5935 (2010).
25. Dengler, V. L., Galbraith, M. D. & Espinosa, J. M. Transcriptional regulation by hypoxia inducible factors. *Critical Reviews in Biochemistry and Molecular Biology* **49**, 1–15 (2014).
26. Walsh, A. J. *et al.* Quantitative optical imaging of primary tumor organoid metabolism predicts drug response in breast cancer. *Cancer Res* **74**, 5184–5194 (2014).
27. Carreau, A., Hafny-Rahbi, B. E., Matejuk, A., Grillon, C. & Kieda, C. Why is the partial oxygen pressure of human tissues a crucial parameter? Small molecules and hypoxia. *Journal of Cellular and Molecular Medicine* **15**, 1239–1253 (2011).
28. Palmer, G. *et al.* Optical imaging of tumor hypoxia dynamics. *Journal of biomedical optics* **15**, 066021 (2010).
29. Godet, I. *et al.* Fate-mapping post-hypoxic tumor cells reveals a ROS-resistant phenotype that promotes metastasis. *Nature Communications* **10**, 4862 (2019).
30. Kapałczyńska, M. *et al.* 2D and 3D cell cultures - a comparison of different types of cancer cell cultures. *Arch Med Sci* **14**, 910–919 (2018).

31. Ast, T. & Mootha, V. K. Oxygen and mammalian cell culture: are we repeating the experiment of Dr. Ox? *Nature Metabolism* **1**, 858–860 (2019).
32. Sachs, N. & Clevers, H. Organoid cultures for the analysis of cancer phenotypes. *Current Opinion in Genetics & Development* **24**, 68–73 (2014).
33. Thakuri, P. S., Liu, C., Luker, G. D. & Tavana, H. Biomaterials-Based Approaches to Tumor Spheroid and Organoid Modeling. *Advanced Healthcare Materials* **7**, 1700980 (2018).
34. Drost, J. & Clevers, H. Organoids in cancer research. *Nature Reviews Cancer* **18**, 407–418 (2018).
35. Griffith, L. G. & Swartz, M. A. Capturing complex 3D tissue physiology in vitro. *Nature Reviews Molecular Cell Biology* **7**, 211–224 (2006).
36. Sachs, N. *et al.* A Living Biobank of Breast Cancer Organoids Captures Disease Heterogeneity. *Cell* **172**, 373-386.e10 (2018).
37. Saglam-Metiner, P., Gulce-Iz, S. & Biray-Avci, C. Bioengineering-inspired three-dimensional culture systems: Organoids to create tumor microenvironment. *Gene* **686**, 203–212 (2019).
38. Nguyen-Ngoc, K.-V. *et al.* 3D Culture Assays of Murine Mammary Branching Morphogenesis and Epithelial Invasion. in *Tissue Morphogenesis: Methods and Protocols* (ed. Nelson, C. M.) 135–162 (Springer New York, 2015). doi:10.1007/978-1-4939-1164-6_10.
39. *Organoid Research Techniques Evolution and Applications*. (Wiley Periodicals, Inc., 2019).
40. Walsh, J. C. *et al.* The clinical importance of assessing tumor hypoxia: relationship of tumor hypoxia to prognosis and therapeutic opportunities. *Antioxid Redox Signal* **21**, 1516–1554 (2014).

41. McMurtrey, R. J. Analytic Models of Oxygen and Nutrient Diffusion, Metabolism Dynamics, and Architecture Optimization in Three-Dimensional Tissue Constructs with Applications and Insights in Cerebral Organoids. *Tissue Engineering Part C: Methods* **22**, 221–249 (2015).
42. Jin, M.-Z. *et al.* Organoids: An intermediate modeling platform in precision oncology. *Cancer Letters* **414**, 174–180 (2018).
43. Wagner, B. A., Venkataraman, S. & Buettner, G. R. The rate of oxygen utilization by cells. *Free Radic Biol Med* **51**, 700–712 (2011).
44. Jardé, T. *et al.* Wnt and Neuregulin1/ErbB signalling extends 3D culture of hormone responsive mammary organoids. *Nature Communications* **7**, 13207 (2016).
45. Hubert, C. G. *et al.* A Three-Dimensional Organoid Culture System Derived from Human Glioblastomas Recapitulates the Hypoxic Gradients and Cancer Stem Cell Heterogeneity of Tumors Found In Vivo. *Cancer Res* **76**, 2465 (2016).
46. Li, X. *et al.* Oncogenic transformation of diverse gastrointestinal tissues in primary organoid culture. *Nature Medicine* **20**, 769–777 (2014).
47. Cheung, K. J., Gabrielson, E., Werb, Z. & Ewald, A. J. Collective Invasion in Breast Cancer Requires a Conserved Basal Epithelial Program. *Cell* **155**, 1639–1651 (2013).
48. Fenner, J. *et al.* Macroscopic Stiffness of Breast Tumors Predicts Metastasis. *Scientific Reports* **4**, 5512 (2014).
49. Qiu, G.-Z. *et al.* Reprogramming of the Tumor in the Hypoxic Niche: The Emerging Concept and Associated Therapeutic Strategies. *Trends in Pharmacological Sciences* **38**, 669–686 (2017).

50. Okkelman, I. A., Foley, T., Papkovsky, D. B. & Dmitriev, R. I. Live cell imaging of mouse intestinal organoids reveals heterogeneity in their oxygenation. *Biomaterials* **146**, 86–96 (2017).

51. Verbridge, S. S. *et al.* Oxygen-controlled three-dimensional cultures to analyze tumor angiogenesis. *Tissue Eng Part A* **16**, 2133–2141 (2010).

52. Cheema, U., Brown, R. A., Alp, B. & MacRobert, A. J. Spatially defined oxygen gradients and vascular endothelial growth factor expression in an engineered 3D cell model. *Cell Mol Life Sci* **65**, 177–186 (2008).

53. Shamir, E. R. & Ewald, A. J. Three-dimensional organotypic culture: experimental models of mammalian biology and disease. *Nature Reviews Molecular Cell Biology* **15**, 647–664 (2014).

Shyanne Salen

ssalen1@jhu.edu | 610-790-4306 | 2933 Saint Paul Street, Baltimore MD 21218

Education

Johns Hopkins University — Baltimore, MD
MSE in Chemical and Biomolecular Engineering — *August 2018 - Converted to Ph.D. June 2019*
Ph.D. in Chemical and Biomolecular Engineering — *June 2019 - Present*

Bucknell University — Lewisburg, PA
Bachelor of Science in Chemical Engineering — *August 2014 - May 2018*

GPA: 3.4/4.0

Research Experience

Johns Hopkins University — Baltimore, MD

Hypoxia-Induced Suicide Gene Therapy — *June 2019 - Present*

- Generated several breast cancer cell lines to express E. coli codA via lentiviral delivery, which encodes cytosine deaminase, under hypoxia. The plasmid design included the addition of HRE (hypoxia responsive elements) and an oxygen dependent domain.
- Conducted drug studies using cytosine deaminase to convert the prodrug 5-FC to the chemotherapy 5-FU. Performed Presto Blue viability assay, crystal violet staining, IF-staining, and image analysis and quantification.

The role of Hypoxia in Tumor Organoids — *October 2018 - Present*

- Optimized a method for culturing breast cancer tumor organoids derived from a novel transgenic mouse model that fate-maps hypoxic cells
- Analyzed hypoxia based on a novel color switching system through fluorescence microscopy, flow cytometry, and RNA analysis
- Optimized a method for culturing breast cancer tumor organoids derived from a novel transgenic mouse model that fate-maps hypoxic cells
- Harvested tumors from mouse models for cell and organoid culture
- Developed the procedure for generating cell lines from harvested mouse tumors

Bucknell University — Lewisburg, PA

Pharmaceutical Development and Crystallization Research — *January 2017-May 2018*

- Worked with a spray dryer to create particles of glutaric acid and analyze how concentration effects size, morphology, and crystallinity of the particles for pharmaceutical tablet development
- Worked with a team of 4 students using a vibrating orifice aerosol generator (VOAG) and a spray dryer to create amorphous particles from dicarboxyl acids to increase the bioavailability of active pharmaceutical ingredients

Course Work

- Thermodynamics, Statistical Mechanics, and Kinetics — Fall 2018
- Interfacial Science with Application to Nanoscal Systems — Fall 2018
- Molecular Immunoengineering — Fall 2018
- Transport Phenomena in Practice — Spring 2019
- Introduction to Polymeric Materials — Spring 2019
- Software Carpentry — Spring 2019
- Metabolic Systems Biotechnology — Fall 2019

Mentoring Experience

- Chioma Ekwunazu, STEP-UP Internship Program — Summer 2019
- Harsh Oza, Biotechnology Master's Student — Fall 2020-Present

Work Experience

Berkshire Systems Group, Inc. Reading PA

Summer Inspection Technician Support *June 2017-Aug 2018*

- Worked with a team of inspection technicians to diligently and efficiently inspect and test commercial fire alarm systems to ensure proper operating in compliance with National, State, and Local Fire Protection Codes and Standards
- Documented test results of all components and list any deficiencies
- Troubleshooted problems in the field to ensure full operation of life safety systems

Berkshire Systems Group, Inc. Reading PA

Summer Sales Support *June 2014-August 2016*

- Aided in conversion of software by working with all departments to provide a efficient transition process
- Created project submittals and Operation and Maintenance Manuals for fire alarm, card access, video surveillance, and sound communication systems
- Implemented new software for creating submittals and operation manuals
- Created instruction manual for other employees to properly use the new custom software

Bucknell University Lewisburg, PA

Residential Advisor *August 2015-May 2018*

- Enforced rules and regulations to ensure the safe and smooth operation of the residence hall
- Mediated interpersonal problems between residents

Leadership Experience

- ChemBE Graduate Student Liaison Committee, Member — Fall 2018-Present
- American Institute for Chemical Engineers (AIChE), Member — Spring 2015-Present
- Society of Women Engineers (SWE), Member — Fall 2014-Present
- Head Coach for Girls on the Run — Fall 2017-Spring 2018
- Chi Omega Sorority Member, Philanthropy: Make-a-Wish Foundation — Fall 2015-Spring 2018

Skills

- **Laboratory**:
  - Mammalian Cell Culture
  - Organoid Generation and Culture
  - Spheroid Culture
  - Mammosphere Assay
  - Mouse Derived Cell Line Generation
  - Immunofluorescence Staining
  - Fluorescence Microscopy
  - Drug Studies
  - Cloning
  - Plasmid Amplification and Purification
  - Lentiviral Infection and Delivery
  - Animal Work: Mouse - Tumor Implication and Necropsy
  - RT-PCR
  - Confocal Microscopy
  - Flow Cytometry
  - Extraction and RNA isolation
  - Western Blot
  - Cryosectioning
  - Genotyping
- **Computer Programs**:
  - Python
  - GraphPad
  - Matlab
  - Microsoft Office
  - Simulink
  - Flow Jo
  - Imaris
  - Image J
  - LaTeX
  - Gen5 - Biotek